AIAA 2000-2383

# IMPLEMENTATION OF THE WICS WALL INTERFERENCE CORRECTION SYSTEM AT THE NATIONAL TRANSONIC FACILITY

Venkit Iyer, Lockheed Martin
Joel L. Everhart, NASA Langley Research Center
Pamela J. Bir, ViGYAN, Inc.

NASA Langley Research Center
Hampton, VA 23681

and

Norbert Ulbrich, Sverdrup Technology, Inc.
NASA Ames Research Center
Moffett Field, CA 94035

**21st AIAA Aerodynamic Measurement Technology and Ground Testing Conference**
19-22 June 2000 / Denver, CO

AIAA 2000-2383

# IMPLEMENTATION OF THE WICS WALL INTERFERENCE CORRECTION SYSTEM AT THE NATIONAL TRANSONIC FACILITY

Venkit Iyer*, Lockheed Martin
Joel L. Everhart†, NASA Langley Research Center
Pamela J. Bir‡, ViGYAN, Inc.
and
Norbert Ulbrich§, Sverdrup Technology, Inc.

## ABSTRACT

The Wall Interference Correction System (WICS) is operational at the National Transonic Facility (NTF) of NASA Langley Research Center (NASA LaRC) for semispan and full span tests in the solid wall (slots covered) configuration. The method is based on the wall pressure signature method for computing corrections to the measured parameters. It is an adaptation of the WICS code operational at the 12 ft pressure wind tunnel (12ft PWT) of NASA Ames Research Center (NASA ARC). This paper discusses the details of implementation of WICS at the NTF including tunnel calibration, code modifications for tunnel and support geometry, changes made for the NTF wall orifices layout, details of interfacing with the tunnel data processing system, and post-processing of results. Example results of applying WICS to a semi-span test and a full span test are presented. Comparison with classical correction results and an analysis of uncertainty in the corrections are also given. As a special application of the code, the Mach number calibration data from a centerline pipe test was computed by WICS. Finally, future work for expanding the applicability of the code including on-line implementation is discussed.

## INTRODUCTION

The National Transonic Facility (NTF) was designed for high Reynolds number testing in a cryogenic, pressurized environment with slotted tunnel walls to alleviate transonic wall interference effects. Recently, the facility has developed the capability to run tests on large high-lift models at subsonic speeds with the tunnel wall slots covered. The need for an accurate and reliable method to compute wall interference corrections for full span and semispan testing under solid wall conditions became apparent. Stringent accuracy requirements on corrected equivalent free-air values of measured parameters limit the use of classical corrections except at low lift conditions.

The wall interference code WICS[1] is based on the wall signature method of Hackett[2] to compute corrections for solid-walled tunnels. It has been operational at the Ames 12 ft pressurized wind tunnel for several years. In this method, the aerodynamic test article is represented by a discrete number of singularities whose strengths are computed by a global fit of the tunnel wall pressures and the measured forces and moments. Subsequently, the code computes the averaged blockage and AOA corrections based on interpolation from databases of perturbation velocities or influence coefficients. These corrections are then applied to the tunnel parameters to approximate the equivalent free-air flow field. In addition, the code provides the wall interference variation in the vicinity of the model (which is not obtainable from simpler classical methods). The advantage of the method is that it is fast, robust and suited for real-time application; therefore, it was selected for implementation at the NTF.

The method is currently operational at NTF and has been successfully applied to recent semispan and full span tests. This paper presents a summary of tunnel calibration activities, WICS implementation for semi-span and full span tests, and a sample of results obtained. Work reported here falls under one of the

---

* Aeronautical Engineer, Senior Member AIAA.
† Research Engineer, Senior Member AIAA.
‡ Research Engineer, Member AIAA.
§ Senior Aerodynamicist.

four main areas of the NTF characterization effort described in Reference 3.

## NTF IMPLEMENTATION ISSUES

Conversion of WICS from the ARC 12 ft PWT implementation to an NTF version required the completion of several related tasks. Tunnel empty calibration under closed slots condition and installation of a new upstream reference pressure measurement system and calibration were done. The new high accuracy flow reference system (FRS) became necessary since the plenum reference pressure system used for slots open tests is not valid for closed slots applications.

Supporting tests were conducted to calibrate the tunnel at empty condition as well as with a centerline pipe, and with the model support in place (for full span models). The centerline pipe calibration provided the Mach number correction using the FRS system. This Mach number correction provides the correct tunnel reference velocity and Mach number at model center of rotation.

An interface program was developed to handle various facility-dependent conversions for WICS. Modifications to the WICS code itself were done to address issues such as tunnel geometry, support geometry and kinematics, image plane differences, tunnel calibration and post-processing. Figure 1 shows a concise description of changes made for semispan application as an example.

Since the wall signature is a key input for WICS, the electronically-scanned pressure (ESP) measurements from the tunnel wall ports are required at the same level of accuracy as the model measurements. An ESP health monitoring system was put in place to monitor reference pressure ports and signal when re-calibrations were necessary. The wall ESP system was held to a 0.1% of full scale standard. This translated into a $\pm$ 0.0025 psi variance for the differential pressure measurements on the wall ESP modules. For example, averages of 10 samples of reference pressures were taken every 15 seconds and used to alert a calibration drift. The measured wall data were also displayed and monitored during the test to ensure quality wall signature inputs into WICS.

Data quality is an important issue for the tunnel empty data since it serves as the basis for the tare corrections to the closed slot tunnel tests. Detailed analysis of the quality and consistency of tunnel empty data was performed to remove outliers and identify calibration drifts. Scaling methods were employed to improve the quality of high noise data under low Q conditions. The tunnel empty database currently consists of a test matrix of 12 points with 4 Mach numbers (0.1, 0.2, 0.3, 0.45) and 3 total pressure values ($P_T$ = 15, 52, 89 psi). The calibration database for the model support also covers the above Mach number and $P_T$ range with the additional variable of sting support system angle of attack. Future calibrations will expand this database to a larger envelope.

For semispan tests, the original WICS code was designed to be applied to a near-circular geometry with an image plane and with the model mounted vertically. At NTF, the image plane is on the far side wall (i.e., the left wall when looking from upstream of test section) and the model is mounted horizontally. The corresponding changes have been made in the code.

The original code assumes the 12ft PWT wall layout, consisting of 8 rows on the wall with each row having equal number of equally distributed ports. At NTF, more rows are available and a subset of the entire wall set is used to input the wall signature. The database generation program used for WICS-NTF is designed to accommodate specific port selections and specification of fictitious ports to fit the fixed number of ports per row requirement in the code. The fictitious ports are excluded during computation of the corrections. The implementation of these changes led to the development of a new pre-processing procedure to prepare data for running the code.

Since the NTF tunnel has a rectangular cross-section, the method of images (MOI) can be used to generate the perturbation velocity databases (see next section for more details). This is much simpler than the original method of using a modified panel code to generate them. A new program was developed to generate the databases in a format identical to the previous modified PMARC[4] panel method. The resulting databases are more accurate and has none of the convergence problems sometimes found in the panel method.

Post-processing of WICS-NTF output is done using TECPLOT® graphics. The corrections and other diagnostic data are output in files in TECPLOT® format. A number of plot scripts using data extraction programs and layout files are available to quickly present data in a number of standard plots. The code was modified to implement these changes.

Figure 2 shows a flow chart of processing operations for WICS-NTF. The tunnel calibration and database generation processes are done prior to a test. Current implementation is for a post-run or end-of-shift

computation of corrections; post-point, on-line application is in development.

## PERTURBATION VELOCITY DATABASES

The first step in WICS application is the computation of databases of perturbation velocity. This CPU-intensive task is completed prior to the test based on tunnel geometry, distribution of wall orifices, model dimensions and Mach number range. Reference 1 gives a complete description of the underlying theory. A short summary is given here.

Two types of singularities are considered viz., a source (or sink) and a semi-infinite line doublet. In WICS, depending on the location and size of the model, these singularities are placed at several discrete locations in the tunnel. The singularity grid used for the database is such that it encompasses the real time positions of the model singularities. The MOI code is run repeatedly with the singularity at each one of the grid locations. Prandtl-Glauert scaling for compressibility $\beta = \sqrt{1 - M_\infty^2}$ is applied to the panel geometry and solutions.

The first type of database for WICS consists of a three-dimensional array of the velocity signature of individual singularities (placed at singularity grid locations) at each tunnel wall orifice location. This database is used to fit the real-time wall signature by superposition of elemental signatures, obtained by interpolation. The quantity stored in the database is $u_p$, the perturbation velocity in the axial direction caused by an individual singularity of unit strength at a certain wall orifice, normalized by the tunnel reference velocity. Typically at NTF, 360 ports are selected for use in WICS (12 rows of 30 ports each, some of which may be turned off for semispan testing). In the method of images, $u_p$ corresponds to the direct effect of the singularity at the wall orifice plus the effect due to an infinite number of images of the singularity from the four walls. This is equivalent to enforcing a tangency boundary condition at the wall. Since the port selection may vary from test to test, a master database for all the available ports is generated first; an extraction routine is subsequently run to customize the database for a specific number of ports.

The second type of database consists of elemental interference velocities, which is used in WICS to compute the actual wall corrections. This database is obtained as an array of perturbation velocity components ($u_i$, $v_i$, $w_i$) from the flow field solution at tunnel interior points. These are wall-induced velocities corresponding to the sum of effects due to the images only (the direct contribution of the singularity itself is not included). These normalized wall interference velocity components in the three Cartesian directions are computed at various locations encompassing the model. The flow field locations belong to a grid defined as the reference grid (which can be distinct from the singularity grid). In WICS, the wall interference at a given real-time reference point is obtained by a tri-linear interpolation from this database. The $u_i$ component contributes towards blockage and $w_i$ contributes towards upwash corrections (for full span models, $v_i$ contributes towards the sidewash corrections if the model is rolled or yawed).

## WALL SIGNATURE FOR WICS

The rows and ports selection for WICS is based on the constraints of the existing tunnel walls orifice layout in the NTF and the requirement that the WICS code be provided a wall signature of adequate resolution. Figure 3 shows the current wall ports layout for NTF, and an example sub-set of the port selections used for WICS (shown as filled circles). Figure 4 shows the relative location of the rows in the Y-Z plane looking from upstream. The number of ports used dictates the size of the database and the time required to compute corrections per data point. Also in WICS, since each port signature contributes equally to the final fit, it is important to use ports that are most significant in defining the wall signature. In the absence of yaw and roll, the top and bottom walls capture the interaction effect adequately. Additionally, the side wall middle rows were also included to bring in side wall asymmetry influences. Ports on the far side wall are turned off for the semispan case since they are on the reflection plane. A hookup table was employed in an interface program to select or de-select specific rows and ports for WICS based on pre-processing of the wall data. For code implementation ease, a fixed number of ports per row was desirable; hence a few fictitious ports were added to some rows (which were flagged to 'off' status in the input).

The starting point in processing tunnel data is a filter program that reads in the test data with tunnel Mach number calibration corrections incorporated. This program scans the test data, removes wind-off points and separates points belonging to individual runs into separate data files. The wall pressure coefficients are converted to corresponding velocity ratios ($V/V_{ref}$), where V is the axial velocity from measured wall pressures obtained from isentropic flow and $V_{ref}$ is the calibrated tunnel reference velocity, as obtained from the FRS Mach number and the centerline pipe data. The filter program is run for test data as well as the empty tunnel data.

Subsequently, an interface program is run to produce files in the WICS input format. The following data extraction and conversion takes place in the interface program: test, run, point information; run parameters in the proper units ($P_T$, $\rho_{ref}$, $V_{ref}$, $M_{ref}$, $Q_{ref}$); point data (AOA, lift, drag and pitching moment) in the proper units; wall orifice values of ($V/V_{ref}$) for the 360 selected ports with setting of good or bad flags for the ports based on analysis of data.

Note that the port flags for empty tunnel data and a given test run data set are combined so that the final 'on' status of a port is possible only if both data set flags agree. This is to ensure that subtraction of tunnel empty wall signature is done properly in WICS. For full span tests, the model support calibration data and interference results are additionally required.

## THE WICS CORRECTION METHODOLOGY

Details of theory, formulation and implementation of WICS are given in References 1 and 5. Here, we present a summary relevant to the NTF semispan version. Additional considerations for full span models are also noted.

After reading the test data and empty tunnel data, the code does an interpolation from the empty tunnel data to obtain the empty tunnel signature exactly corresponding to each test point Mach number and $P_T$. Subsequently, this signature is subtracted from the test point values thereby eliminating specific wall orifice variations, tunnel geometry and tunnel wall boundary layer effects. Figure 5a shows a contour plot for this 'tared' wall signature at the top and bottom walls for one representative test point.

The problem now reduces to one of computing the strength of the singularities representing the model by superposition of the effect of each individual singularity. Since the number of wall orifices is usually much more than the number of unknowns, the system is over-specified and hence lends itself to a least square fitting procedure.

The strength of the wing doublets as a group can be directly computed from the measured lift from the Kutta-Joukowski formula[6]. If the model has a tail surface, another row of doublets is defined at the tail 1/4 chord line to represent the tail lifting effect. In this case, the pitching moment is also used in the equation to determine the strength of the tail group of line doublets. Once the doublet strength as a group is established, the distribution of strengths of individual doublets in the span direction is based on the input (or optionally, computed) weight factors which defines the wing loading.

The cumulative wall signature of the line doublets is then calculated. The perturbation database type 1 for doublets is used here for interpolation depending on the real time position of each doublet singularity. Linear addition of effect due to each singularity yields the combined effect due to doublets. The resulting wall signature is then subtracted form the 'tared' wall signature. The remaining portion of the signature is due to the blockage effect from the model volume and from the wake (represented by sources and sinks). Again, grouping of singularities results in two unknowns viz., strength of the source-sink pair and the combined strength of the wake sources. These two unknowns are determined in a least square fitting procedure such that the computed or 'fit' signature is the best fit of the wall signature in a global sense. Figure 5b shows a contour plot of the 'fit' signature (with the effect of doublets added back on), which should be a good approximation to the real signature shown in Figure 5a.

Note that WICS does not compute the fit row by row; the fit is performed in a global sense. The advantage of this approach is that a few bad ports do not adversely affect the computation. The code has a quality check of the wall signature, which identifies and discards outliers in a second pass (based on $3\sigma$ limits obtained from the fit in the first pass).

Finally, once all the singularity strengths are computed, interpolation from the database type 2 is used to compute corrections at any location in the flow field within the reference grid. The code also does a straight or weighted averaging of the corrections along the actual fuselage axis, wing 3/4 chord line, and other input reference lines to determine mean corrections. If the axial component of the averaged interference field is $u_i$ and the $V_{ref}$ is the measured tunnel reference velocity, then blockage factor (including solid and wake blockages) is defined as $\varepsilon = u_i / V_{ref}$. If $M_{ref}$ is the measured tunnel reference Mach number and $Q_{ref}$ the dynamic pressure, the Mach number and dynamic pressure corrections are computed to first order accuracy as

$$\Delta M = M_{ref}\,\varepsilon\left(1+\frac{\gamma-1}{2}M_{ref}^2\right)$$

$$\Delta Q = Q_{ref}\,\varepsilon\left(2-M_{ref}^2\right)$$

Similarly, for a model mounted horizontally, if $w_i$ is the averaged vertical component of the interference field, the angle of attack correction is computed as

$$\Delta\alpha = \tan^{-1}\left(\frac{w_i}{V_{ref}}\right)$$

In addition to these average corrections, local values of corrections along different cutting planes in the model vicinity are also computed. This is useful for producing contour plots of corrections, which helps in assessing how good the averaging is in the calculation of mean corrections. These contour plots will aid aerodynamic analysis and may reveal possible problem areas, such as premature wing stall due to wall effects.

Application to full span models additionally takes into account the interference caused by the support structure. At NTF, this involves an arc sector located about 13 ft downstream of the model center of rotation, and the model support sting. Calibration data of the support system at various values of Mach number, total pressure and angle of attack is used to pre-compute the resulting interaction. This calibration data is also used for 'taring' of the signature, similar to the tunnel empty signature for semispan models. By using the principle of superposition, the interaction due to model plus sting is obtained by adding the support system interaction at identical conditions to the model only corrections. This involves the generation of and interpolation from a separate perturbation velocity database for the support geometry. The current database assumes a straight model sting. Additional calibrations will be required if there are changes in the supporting structure.

## WICS SINGULARITY DISTRIBUTION

In addition to test data, tunnel empty calibration data, and the perturbation velocity database, the code requires the model singularity distribution and weight factors for computing the individual singularity strengths from a computed combined strength. The singularity distribution used to simulate the effect of the model on the tunnel walls, and the wall on the flow field, is based on the use of a source-sink pair to represent solid blockage, a row of semi-infinite line doublets to represent the lifting effects, and a number of sources at separation locations to represent the wake blockage. The distribution is specified on the model at zero angle of attack and moves with the model. By fixing the singularities spatially in groups of source-sinks, doublets and sources, the solution procedure simplifies to one of determining their combined strengths. The number of unknowns is effectively reduced to two (the doublet strengths are determined directly from the measured lift, as given previously).

The location and distribution of singularities are based on certain "rules of thumb". The source-sink pair is placed along the fuselage axis (at the reflection wall for a semispan model). The source is placed one mean fuselage radius downstream of the nose of the fuselage and the sink of equal strength is placed one mean fuselage radius upstream of the tail end of the fuselage; this represents an equivalent Rankine body. Sources of equal weights are placed at locations where separation is expected. Line doublets representing a lift distribution are usually placed along the 1/4 chord line of the wing; the weights can be prescribed by a spanwise distribution (such as elliptic), or computed internally using lifting surface theory. Usually a total of 10 to 15 singularities is sufficient.

It is to be noted that this strategy works well because WICS tries to match the far field effect of the singularities at the wall. Similarly, WICS corrections are computed at model locations relatively far away from the specified signature at the walls; hence this is also a far field effect. Experience has demonstrated that precise location of the singularities is not an important factor in the magnitude of the corrections.

Figures 6a and 6b show views of the singularity distribution used for a representative semispan model and a full span model. For the semispan case, a source-sink pair is placed at the image plane for symmetry. Two sources are placed at the flap trailing edge to capture the wing wake effect and a row of equispaced line doublets is placed along the 1/4 chord line. For the full span case, additional singularities are placed at the horizontal and vertical tails.

## APPLICATION OF WICS-NTF TO SEMISPAN TESTS

Application of the NTF version of WICS is presently done off-line in an end-of-shift mode. An off-line data reduction program merges, averages and reduces raw data and outputs the results in a standard file format. The Mach number calibration correction specific to the reference pressure measuring system used is included in this processing. Force and moment parameters are based on the uncorrected, stability axis-oriented values. This output is the starting point for WICS processing. The data is then run through a filter program and an interface program to extract data required for WICS and present them in the required format. A number of script-based utilities have been developed to accomplish WICS runs and graphic post-processing for a specific run or a number of runs. Final WICS corrections are presented in a standard output file or through TECPLOT®-based graphic output. Details of the processes involved in applying WICS-NTF are given in Reference 7.

We present here results from a representative run of a large (wing reference area / tunnel cross-section area of 0.098) high-lift semispan model at Mach 0.2 and a dynamic pressure Q of 2.4 psi. The AOA range was –5 to 24.

The most important indication of how accurate the WICS corrections are, can be obtained by examining how well the raw wall signature is matched by WICS. The contour plots already presented in Figures 5a, 5b give an overall picture of the real wall signature and the WICS least square fit. In Figure 7 we present a closer look at the comparison for each of the 11 wall rows used in this semispan case. The point corresponding to AOA of 24 is shown here. The wall signature is in terms of perturbation velocity increment relative to the tunnel empty baseline and normalized by the reference velocity at model center of rotation. The raw data computed from measured differential pressures using isentropic assumption are shown as filled symbols. Points flagged as 'bad' based on data analysis or pre-set selection criteria are not shown here. For the same points, the WICS-computed wall signature match is shown as solid lines. Since the method uses a global least square solution for the collective input wall signature based on singularity strengths and location, the WICS fit is not to be interpreted as a least square fit in the local sense. Rather, it is a best match result of the wall signature based on measured parameters, tunnel and model geometry, and assumptions of far-field effect and linear potential theory.

The mean corrections relating to blockage (blockage factor $\varepsilon$, $\Delta$-Mach, $\Delta$-Q; averaged along real time fuselage axis) and upwash (weight-averaged $\Delta\alpha$ at the real-time 3/4 chord line) are shown in Figure 8 for the AOA range of –5 to 24. These values can be directly compared with classical corrections for low-lift attached flow conditions (see the section 'Comparison with Classical Corrections' for more details). It is also possible to define other model-fixed or tunnel-fixed reference axes and compute mean corrections along them.

WICS also computes corrections called secondary corrections, which can be applied directly to the uncorrected coefficients $C_L$, $C_D$, and $C_M$. Corrections to $C_L$ and $C_D$ are due to the inclination of the lift and drag force caused by wall interference, and are based on the mean upwash correction at the 1/4 chord line. The correction to the pitching moment takes into account wall induced changes to the streamline curvature and the shift of center of pressure. Drag coefficient correction due to wall-interference induced changes in the horizontal buoyancy is also computed by integrating the variation of blockage along model surface. These corrections are shown in Figure 9.

It is possible to compute local values of corrections at various locations in the tunnel and study their variation along different tunnel-fixed cutting planes in the model vicinity. Contour plots of these local corrections are useful in assessing the assumption of uniformity of the correction implicit in averaging. Figure 10 shows an example of a contour plot of the local upwash corrections in the model region along the 3 planes X=13 (tunnel cross section), Y=4.1 (reflection wall) and Z=0 (horizontal plane). Symbols representing the spatial location of the singularities and their computed strengths are also shown. The span-wise variation of $\Delta\alpha$ as seen in the X-Y plane panel indicates good conformity with the 1/4 chord line, in this case.

## APPLICATION OF WICS-NTF TO FULL SPAN TESTS

The full span test used here as an example is the generic Pathfinder I transport model, adopted as a check standard for the facility. This model is a typically-sized transonic configuration with a wing reference area / tunnel cross-section area of 0.030. The four major differences for the full span case compared to the semi-span case are the model support system and kinematics, the tunnel empty data, the perturbation velocity database and the use of rows from all four walls. Once these changes are accounted for, the procedure to compute corrections is essentially the same for both cases.

At the NTF, the model support system for a full span test consists of a non-metric model sting attached to the arc sector roll drive on one end and the model balance located inside the model on the upstream end. A straight sting is commonly used although other bent stings have been used for various purposes. The model is capable of pitch and roll rotations; a combination of the two is used to achieve yaw rotation. The model kinematics and lift vector direction are important in WICS because the position and orientation of the singularities are based on it. The present version of WICS assumes pitch rotation only.

Since the sting is in the model wake, it is important to 'tare' the full-span test data with an empty tunnel wall signature with the sting alone in the flow at the same conditions. This enables computation of the interference due to the model only if we neglect the second-order effect due to flow interaction between the model and the sting. The tunnel empty calibration database for the full span case thus consists of wall

signature at various $P_T$, Mach number and sting incidence angles. If the interference due to the sting alone is desired, this calibration data can be 'tare'-d against the fully empty tunnel data (used in semispan case) and used as input for a special version of WICS meant for support configuration interference computation. The corresponding database of corrections is also used for linear addition of interference velocities if it is desired to compute test article plus sting interference corrections.

The perturbation velocity database for the full span case is different from the semispan case because of the obvious difference in effective tunnel aspect ratio as well as due to differences in the placement of the singularity and reference grids discussed earlier under the 'Perturbation Velocity Databases' section. Since there is no reflection plane, the wall signature used for WICS can now include rows from the far wall also.

The singularity distribution for the full span model is shown in Figure 6(b). Because of the presence of the tail lifting surfaces, the pitching moment is now required in addition to the lift to compute the effective doublet strength. Figure 11 shows plots of the mean corrections computed for the Pathfinder model. Comparison with Figure 8 shows that the blockage due to the full span model is an at least an order of magnitude less than that of the semispan model. This is consistent with the smaller frontal area and wake of this transport model. Note that while blockage is greatly reduced over that of the semispan model, a significant correction to the angle of attack is still present.

Figure 12 shows a comparison the row-wise signature distribution from the test and WICS. The wall signature is considerably smaller compared to the semi-span case. As a result, the WICS fit has a smaller standard deviation value. In addition, the full span model has a higher aspect ratio than the semispan model and a more conventional pressure distribution on the wing, which leads to a better fit of the wall signature.

## MACH NUMBER CALIBRATION FROM WICS

A special application of the WICS code was made to predict the Mach number variation along the tunnel centerline from the tunnel flow reference system (FRS) measurement location at station X=-2 to the tunnel model reference station X=13. This is typically obtained from a centerline pipe test and applied as a Mach number correction added to the measured reference value to the get the conditions at the model reference station.

The Mach number change from the FRS location to model center location in an empty tunnel occurs due to the boundary layers on the walls which is a function of the Mach number and Reynolds number. Based on the centerline pipe data, the change in reference conditions is expressed as a set of calibration curves $\Delta M=f(M,Re)$. This blockage effect can be modelled in WICS by specifying a number of source-sink-source triples distributed along the centerline (this implicitly assumes symmetry in the signature at the four walls and uniform flow at the tunnel section where the FRS is located). The wall signature from the tunnel empty test is used as input directly into WICS (no 'taring' required) with tunnel reference velocity $V_{ref}$ set to the FRS-based velocity. It is also required to generate a special database of elemental perturbation velocities with the singularity and reference grids positioned along the centerline in a denser distribution. The resulting local values of the Mach number correction is added to the FRS value to get the WICS-predicted Mach number distribution along the centerline.

Figure 13 shows a comparison of the local Mach numbers from centerline pipe data and WICS for the test conditions M=0.45, Q=11 psi (Re=16 million/ft). The centerline pipe data and error bar are from three repeat points at each location averaged from 4 ports, 90° apart. The results from the WICS calculations also correspond to these three repeat points. In order to account for slight differences between the centerline and wall flows at X =-2, the WICS results were shifted by a fixed amount corresponding to the average difference in Mach number at the centerline and wall at the FRS location. A good match of the experimental distribution has been obtained.

The above procedure was repeated for all the points in the tunnel empty data set. Figure 14 shows a plot of the $\Delta M$ values from WICS compared to the experimental calibration values taken at tunnel station 13, the model center of rotation. A good match of the calibration values to within +/-0.0005 in Mach number has been obtained. This application serves as a validation of WICS in addition to the use of it to check the centerline pipe calibration.

## ANALYSIS OF UNCERTAINTY OF CORRECTIONS

It is difficult to assign definite values to the uncertainty in the corrections because the accuracy of corrections is dependent on the method, the measurements and the interference flow field, all of which vary from test to test. The true answer is available only indirectly through test data from models of various scales in

tunnels of varying sizes, which can indicate the trend to the 'free air' solution.

The WICS method makes the assumption that the rotational flow in the vicinity of the wall and in the vicinity of the model are far removed so that the effects of one on the other can be modeled in a lumped fashion. When this is violated (larger models, high values of AOA and semispan image plane issues are examples), the accuracy of WICS tends to be degraded and can be directly seen in the row-wise standard deviation of the WICS fit. The tunnel upwash correction is directly computed from the pitching moment and the lift; the uncertainty in its value is mainly dependent on the approximation used in wing and tail loading distribution. The blockage correction results from the subtraction of the lift-induced effect from the total signature and contains most of the uncertainties resulting from the measurements, the tunnel flow non-uniformity and orifice error. Therefore the blockage corrections have a larger degree of uncertainty in them especially in a model with small blockage and a large lift. Results from WICS at the 12 ft PWT show that the accuracy of the wall signature is a key parameter. In a particular test, the scatter in the blockage predictions was found to increase from +/-0.001 to +/-0.005 if wall pressure ESP modules were not re-zeroed for each change in the dynamic pressure. An indirect verification of blockage correction also is seen from a 12 ft PWT test with a full length flap and a half span flap. The blockage correction decreased for the half-span flap case approximately by half that of the full-span flap when compared to the classical correction value with no flap. Another approach is to systematically perturb the WICS input parameters and find the sensitivity indices; once these are available, the standard deviation of the WICS corrections can be obtained based on input deviations. This work is currently ongoing. This does not address other accuracy issues relating to flow features of a specific test article.

## COMPARISON WITH CLASSICAL CORRECTIONS

An assessment of the predictive capability of the WICS code may be obtained by comparing its results with those given by classical theory. Accordingly, the wind tunnel measurements of the high-lift semispan model were also corrected for wall effects using standard methods presented in Barlow, Rae, and Pope[8], AGARDograph 109[9] and AGARDograph 336[10]. An extended version of Maskell's theory[11] developed by Hackett[12] was used to correct for the separated wake flow generated by the high-lift system. Hackett's two-step extension removes the over-correction tendency of the Maskell theory by separating the wake blockage and wake gradient effects into constituent parts, in lieu of the original combined correction.

Prior to comparing the correction increments, a general discussion of the effect of the tunnel walls on measured data is in order. In solid wall tunnels, the flow is constrained such that an over-acceleration around the model is present. This effect is known as blockage interference; it is a function of the model volume and its wake; and, the correction is to increase the effective tunnel velocity and dynamic pressure, resulting in lower values of the aerodynamic coefficients. The presence of the wake generates two effects. First, the area between the wake and the tunnel walls is constrained and causes an increase in the velocity that is sensed upstream as a change in the flow velocity. This increased velocity is manifested as an additional change in the dynamic pressure known as wake blockage. The second effect is due to the wake-flow velocity gradient over the model. This effect generates a drag correction in the same manner as that due to an empty tunnel gradient. The walls also increase the lift for a given angle of attack, which for a given lift has the corrective effect of increasing the model incidence. In linear flow regimes, this effect is proportional to the lift and it is known as lift interference. Fluid streamlines must be parallel to the tunnel walls in the vicinity of the wall, instead of ballooning around the model as in unconstrained flow. This flattening reduces the curvature of the flow near the model and redistributes the loading, effectively reducing the camber of the model. This re-cambering yields an increment in the pitching moment known as streamline curvature interference.

In classical theory, these tunnel wall interference variations are captured by the appropriate selection of $\varepsilon$, the total blockage parameter; $\delta_0$, the lift interference parameter; and $\delta_1$, the streamline curvature parameter. These parameters are defined as:

$$\varepsilon = \frac{\Delta u}{U_\infty}; \quad \delta_0 = \Delta\alpha \frac{C}{SC_L}; \quad \delta_1 = \Delta\alpha_{SC} \frac{2\beta H}{\bar{c}} \frac{C}{SC_L}$$

where $\Delta u$ is the velocity increment due to blockage, $\Delta\alpha$ is the wall induced increment in angle of attack, $\Delta\alpha_{sc}$ is the wall induced increment due to streamline curvature interference, C is the tunnel cross-sectional area, H is the tunnel height, S is the model reference area, and $\bar{c}$ is the mean aerodynamic chord. When applying classical theory, much latitude exists during the selection of interference parameters. These parameters are determined from charts and equations that are dependent on the specifics of tunnel and model

geometric details, such as the inclusion of corner fillets in the test section area and semispan standoff in the model volume. By reversing the process, output from the WICS code can be used to compute values of the interference parameters. In the present case, because of the wide latitude in parameter selection, the lift interference parameter, $\delta_0$, was selected as 0.11 to match the WICS-computed results of the cruise configuration of this model; $\delta_0$ was thereafter held constant. The streamline curvature parameter was determined as $\delta_1 = 2.135\ \delta_0$ using Reference 9. The blockage $\varepsilon$ was determined using References 8, 11, and 12.

From the previous discussion, it is obvious that tunnel flow conditions, model attitude settings, and aerodynamic coefficients determined from measured loads, all, change with the application of wall interference corrections. In other words, when corrections are applied, data are transformed in measurement space from the point (M, Re, q, $\alpha$, $C_L$, $C_D$, $C_{PM}$) to the correction point ($M_C$, $Re_C$, $q_C$, $\alpha_C$, $C_{LC}$, $C_{DC}$, $C_{PMC}$). This is illustrated in Figure 15 where representative uncorrected measurements are compared with both the "Classical Plus Maskell" (CM) and the WICS corrected measurements. Lift results ($C_L$ vs. $\alpha$) are presented in the upper portion of Figure 15 and drag results ($C_D$ vs. $C_L$) are presented in the lower portion. An examination of the results demonstrates a transformation consisting of a rotation and scaling of the polars from the uncorrected state (circles) to the corrected state (open and filled squares). For example, the uncorrected circle labeled "1" on the drag polar is transformed to the CM-corrected open square labeled "2" and the WICS-corrected filled square labeled "3". In this case, relatively small changes in drag correction occur while large corrections to lift and angle of attack are present, as noted in the upper figure. This is an important concept to remember in the following presentation where total increments between the corrected and uncorrected aerodynamic coefficients are presented.

Total increments between the corrected and uncorrected lift, drag, and pitching moment measurements have been plotted as a function of uncorrected lift coefficient in Figure 16 for the CM and the WICS methods. In each case, the open symbols represent CM theory, while the closed symbols represent that due to WICS. In all cases, the increments vary in a similar and consistent manner, regardless of the correction method; however, significant differences are present. Examining the lift results in Figure 16a reveals a rotation between the curves and a nonlinear spreading of their separation above $C_L$ of 1. When applying classical theory, most of the differences due to rotation can be removed by "judiciously tuning" values read from charts. However, the nonlinear widening reflects differences in the methods and their ability to properly capture the flow physics. The CM theory imposes a mathematical boundary simulation of no flow through the wall, while the WICS theory imposes a reality in the form of a measured pressure boundary. This measured pressure boundary inherently reflects the state of the tunnel geometry and the wall boundary layer, the presence of which has been demonstrated to alleviate both solid wall blockage and the streamline curvature interference[13, 14]. In effect, the tunnel wall boundary layer allows a measure of streamlining as would an adaptive wall tunnel. The WICS code appears to capture these characteristics as evidenced by the reduced total corrections for lift and for pitching moment as seen in Figure 16c. Drag increments presented in Figure 16b compare extremely well at $C_L$ values up to 0.7 where the total correction grows to about 35 drag counts and the difference between the methods is under 3 drag counts. Beyond this, the influence of the flow separation becomes significant and the difference between the methods grows to 40 drag counts at a $C_L$ of 1.3, and even greater at higher lift coefficients. It is unknown which method definitively yields the more correct value. However, at this point, WICS is the more credible solution because of its more realistic boundary condition and because of similar results presented by Rueger in reference 15 where he compared the two "measured-variable" technique with the wall signature method (WICS) and CM corrections. Though not presented, computational results from the WICS code indicate a reduction in blockage interference with increasing Reynolds number. This reduction is consistent with tunnel area changes due to wall boundary layer thinning as Reynolds number increases. Variations in blockage due to Reynolds number can not be assessed using CM techniques.

## FUTURE WORK

On-line implementation of WICS on a post-point basis is a key item for future work. The method is computationally efficient enough to make this possible in near real-time. Each test point contains all the information required for WICS computations; the entire polar is therefore not required (classical corrections for separated wake blockage may require the entire polar). Future work also involves added capability to process tests with roll and hence a change in the lift vector direction. Augmentation of calibration data with additional tests with other support configurations is also required. Additional calibration data is also required to

extend the Mach and Reynolds number range of the current databases. An effort is under way to improve the quality of the wall signature by additional port locations on the near wall, rectification of some of the known problem ports, relocation of ESP modules, and re-plumbing of lines. An analysis of the sensitivity of corrections to turning off different rows is being done. More tests are required to build confidence in the method.

## CONCLUSION

The wall interference code WICS based on the wall signature method has been successfully implemented at the National Transonic Facility. The method uses pre-computed databases of corrections, which helps in fast and reliable computations. The code has been applied to a recent low-speed, high-lift semispan model and a full span model. Analysis of the results indicates that the wall signature is well matched by the code. The global least square nature of the wall signature match results in corrections that are insensitive to isolated bad input data.

## ACKNOWLEDGMENTS

A part of the work reported in this paper was performed under NASA Langley contract NAS1-96014.

## REFERENCES

1. Ulbrich, N., "The real-time wall interference correction system of the NASA Ames 12-foot pressure tunnel," NASA/CR-1998-208537, July 1998.
2. Hackett, J.E., Wilsden, D.J., and Lilley, D.E., "Estimation of tunnel blockage from wall pressure signatures: a review and data correlation," NASA CR-152241, March 1979.
3. Bobbitt, C., Everhart, J., Foster, J., Hill, J., McHatton, R., and Tomek, B., "National Transonic Facility characterization status," AIAA-2000-0293, January 2000.
4. Ashby, D.L., Dudley, M.R., Iguchi, S.K., Browne, L., and Katz, J., "Potential flow theory and operation guide for the panel code PMARC," NASA TM 102851, NASA Ames Research Center, Moffett Field, CA, January 1991.
5. Ulbrich, N. and Boone, A.R., "Real-time wall interference correction system of the 12ft pressure wind tunnel," AIAA 98-0707, January 1998.
6. Ulbrich, N., and Steinle, Jr., F.W., "Semispan model wall interference prediction based on the wall signature method," AIAA 95-0793.
7. Iyer, V., "WICS-NTF User Manual," NTF Internal Report, April 2000.
8. Barlow, Jewel B., Rae, William H., Jr., and Pope, Alan, "Low-Speed Wind Tunnel Testing", 3rd ed., John Wiley and Sons, Inc., New York, 1999.
9. Garner, H. C., Rogers, E. W. E., Acum, W. E. A., and Maskell, E. C., "Subsonic Wind Tunnel Wall Corrections", AGARDograph 109, October 1966.
10. Ewald, B. F. R. (Editor), "Wind Tunnel Wall Correction", AGARDograph 336, October 1998.
11. Maskell, E.C., "A Theory of the Blockage Effects on Bluff Bodies and Stalled Wings in a Closed Wind Tunnel", R&M 3400, November 1963.
12. Hackett, J.E., "Tunnel-Induced Gradients and Their Effect on Drag", Lockheed Georgia Co., Lockheed Engineering Rept. LG83ER0108 Revision 1, Marietta, GA, September 1994.
13. Berndt, S. B., "On the Influence of Wall Boundary Layers in Closed Transonic Test Sections," FAA Rept. 71, 1957.
14. Adcock, J. B. and Barnwell, R. W., "Effect of Boundary Layers on Solid Walls in Three-Dimensional Subsonic Wind Tunnels", AIAA Journal, Vol. 22, March 1984, pp. 365-371.
15. Rueger, M. L., Crites, R. C., and Weirich, R. F., "Comparison of Conventional and Emerging ("Measured Variable") Wall Correction Techniques for Tactical Aircraft in Subsonic Wind Tunnels", AIAA 95-0108, January 1995.

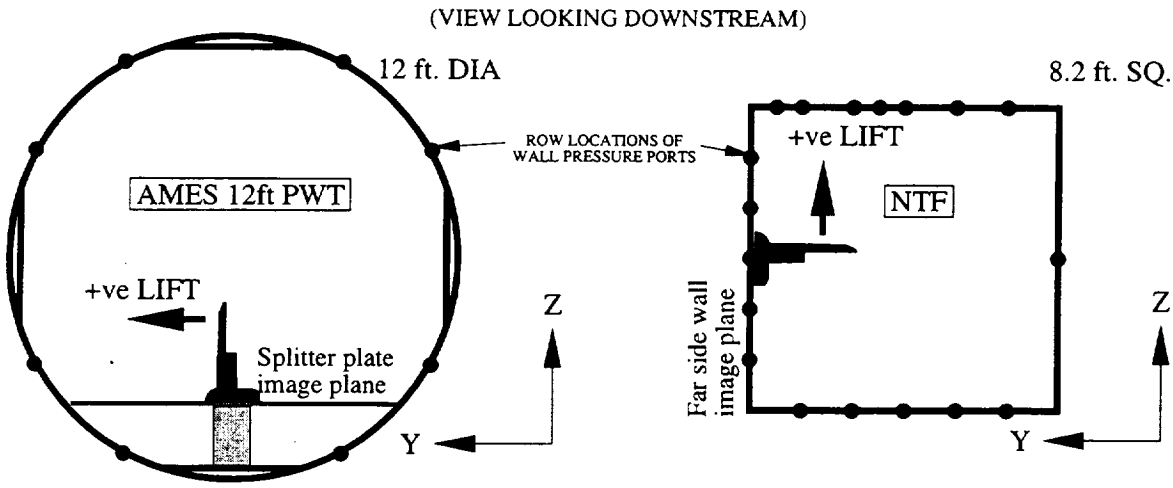


| | AMES 12ft PWT | NTF |
|---|---|---|
| GEOMETRY | Near-circular cross section (12 ft DIA) | Rectangular (8.2 ft SQ.) |
| WALL SYSTEM | 8 rows, 30 ports/row, equally spaced | 16 main rows, unequally spaced |
| MODEL ORIENTATION | Left wing half on image plane, extends in +Z | Left wing half on far side wall, extends in −Y |
| PERT. VEL. DATABASE | Modified PMARC panel code | Code based on Method of Images (MOI) |
| WICS APPLICATION | Real time or off-line | Off-line; interfaces to DAS output |
| POST-PROCESSING | IDL graphics | TECPLOT graphics |

Figure 1. WICS implementation issues at NTF (semi-span model example).

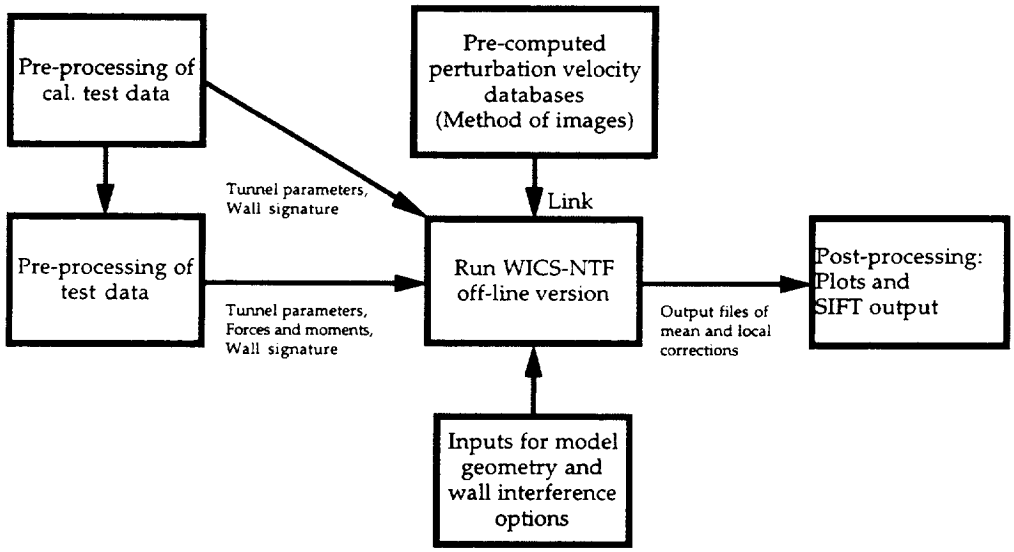


Figure 2. Flow chart of processing operations for WICS-NTF.

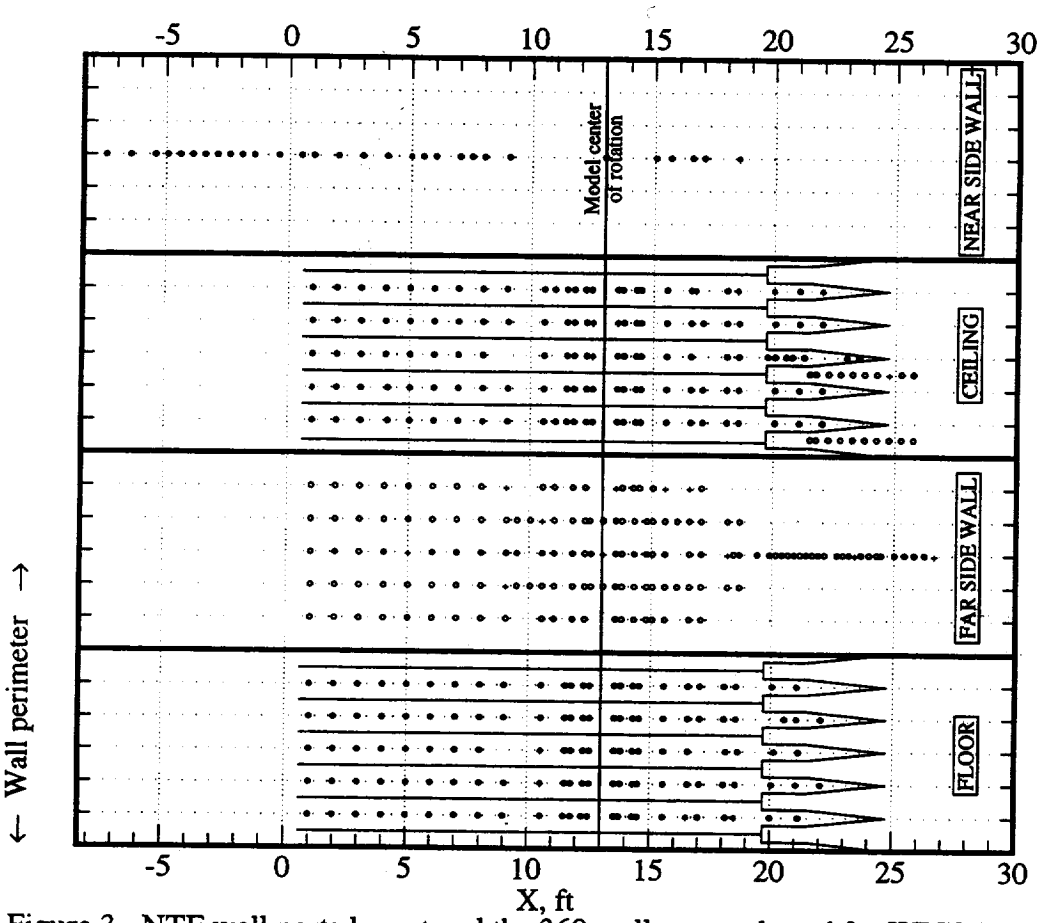


Figure 3. NTF wall ports layout and the 360 wall ports selected for WICS-NTF.
(Open symbol , port is hooked up. Symbol +, port is bad or not hooked up. Filled symbol, port selected for WICS)

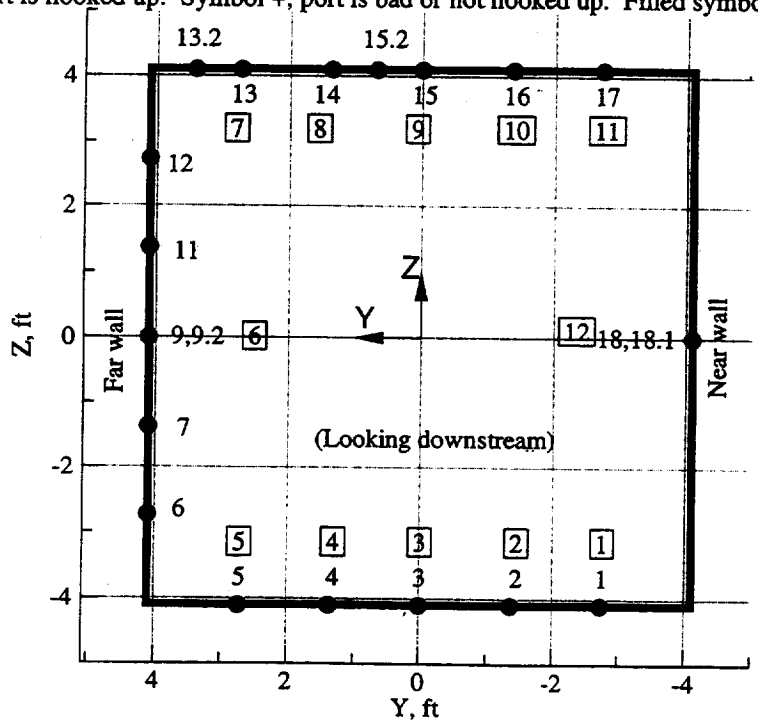


Figure 4. Location of wall ports showing row numbers (WICS row numbers in box outline).

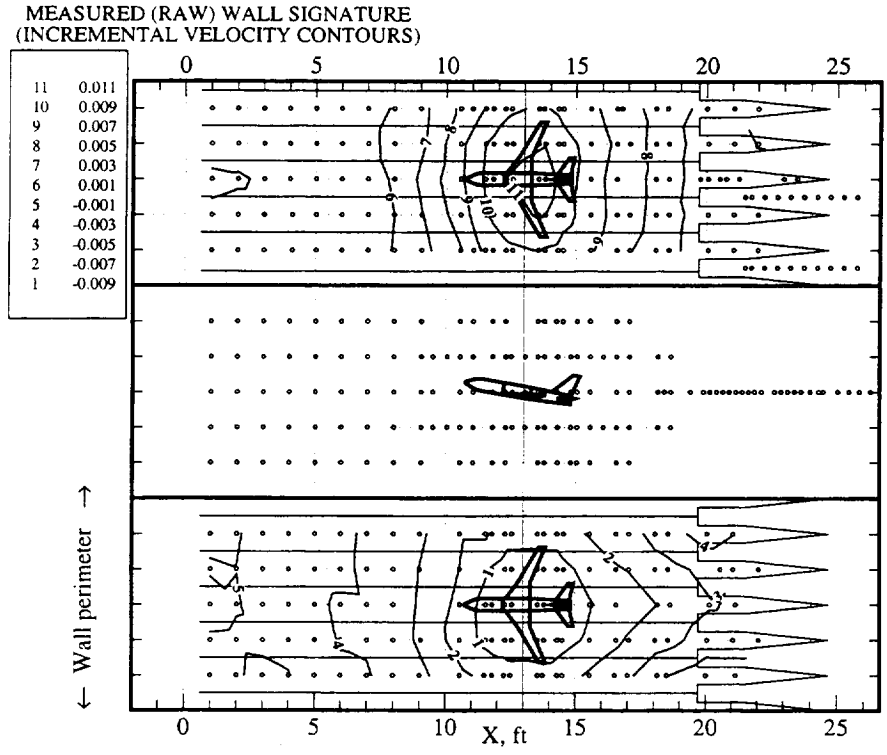


**(a)**

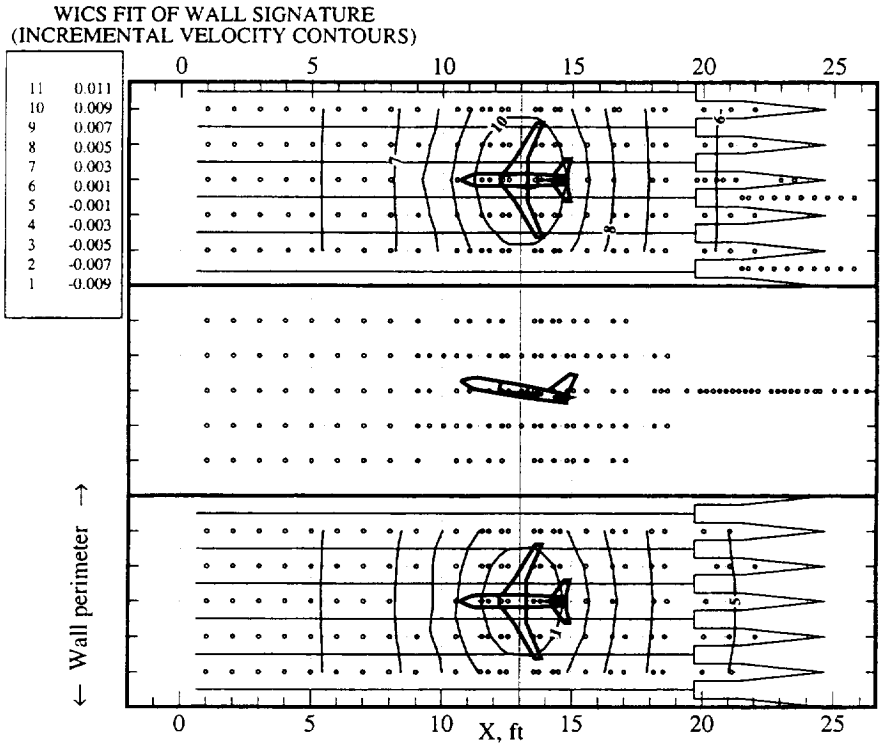


**(b)**

Figure 5. Wall signature from a full span (Pathfinder-I) model at $\alpha$=10° (a) from raw data, (b) from WICS-NTF fit to the raw data.

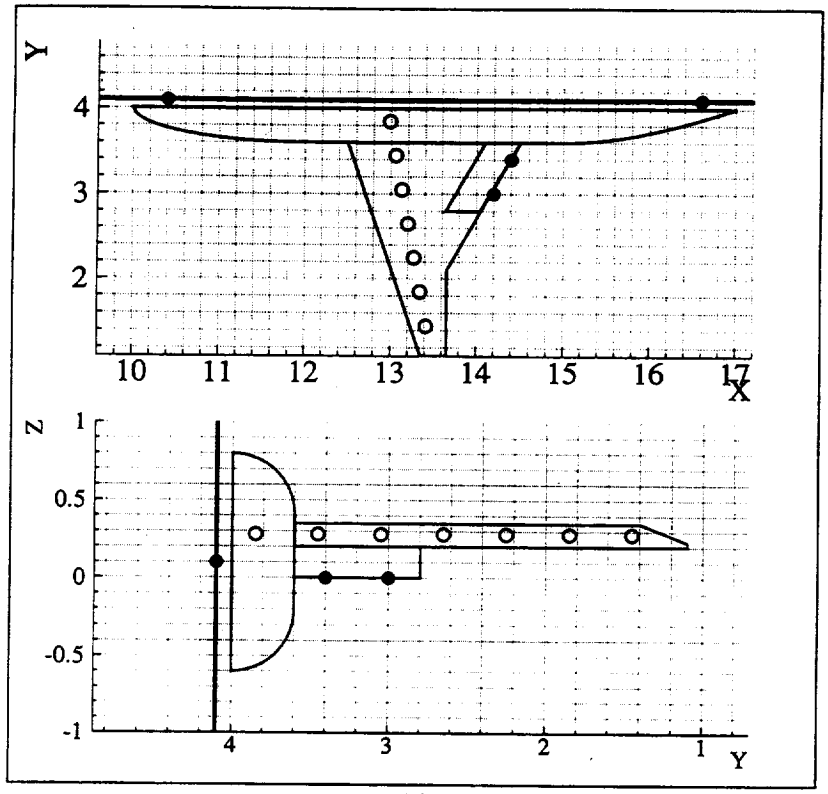


(a)

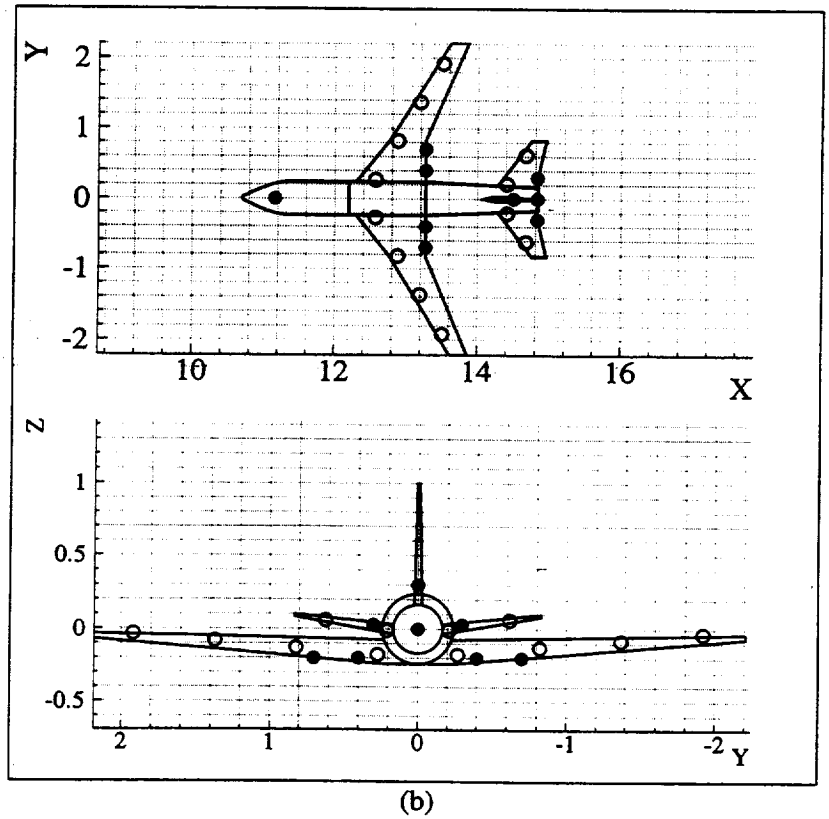


(b)

Figure 6. Singularity distribution and model lines for (a) a semi-span case, (b) full span case; open symbols are semi-infinite line doublets; filled symbols are point sources or sinks.

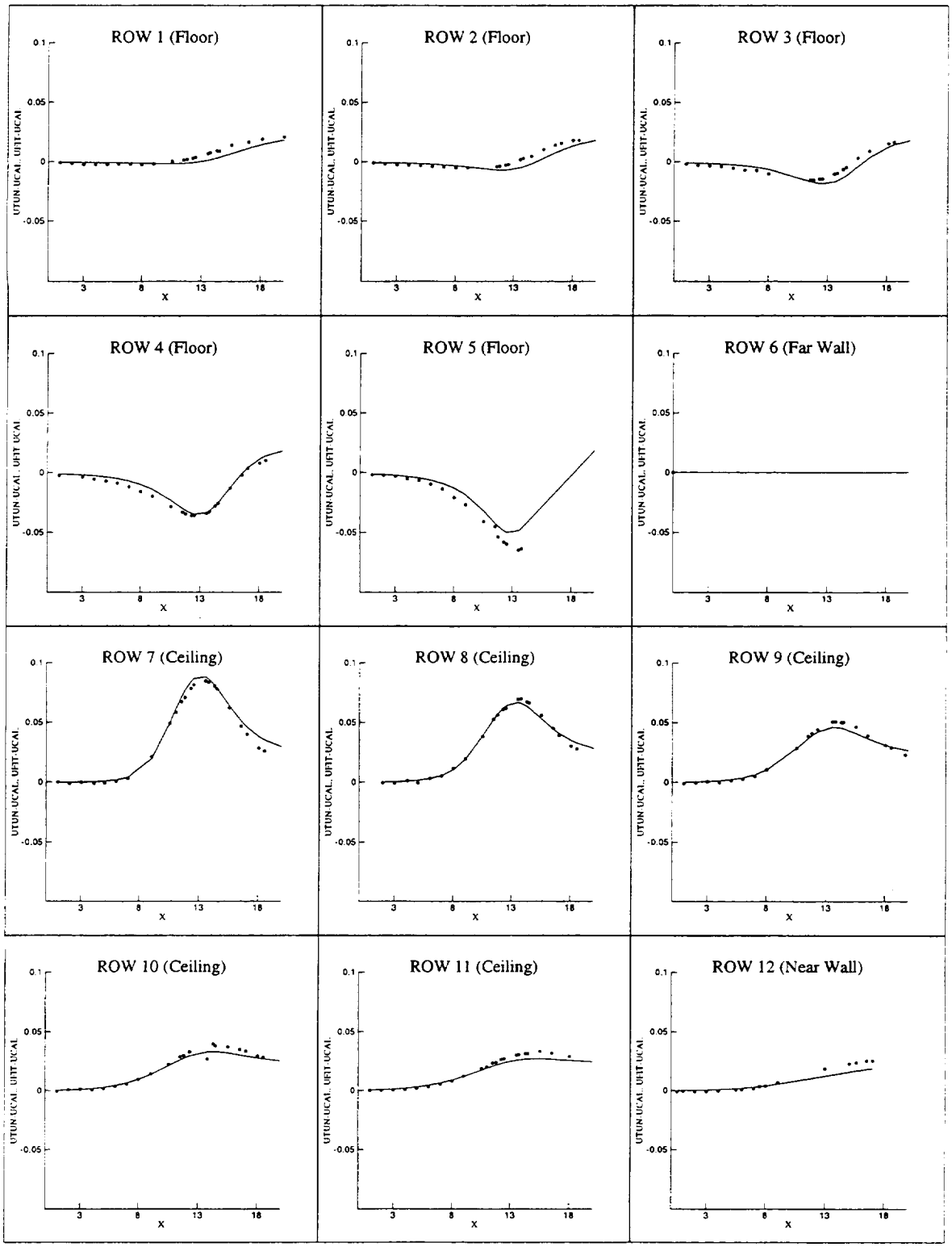


Figure 7. Wall signature, raw data and WICS-NTF fit, semi-span model at AOA=24°.
Symbols: UTUN-UCAL (Raw perturb. vel. minus tunnel empty vel.); Lines: UFIT-UCAL (WICS global fit of UTUN-UCAL).

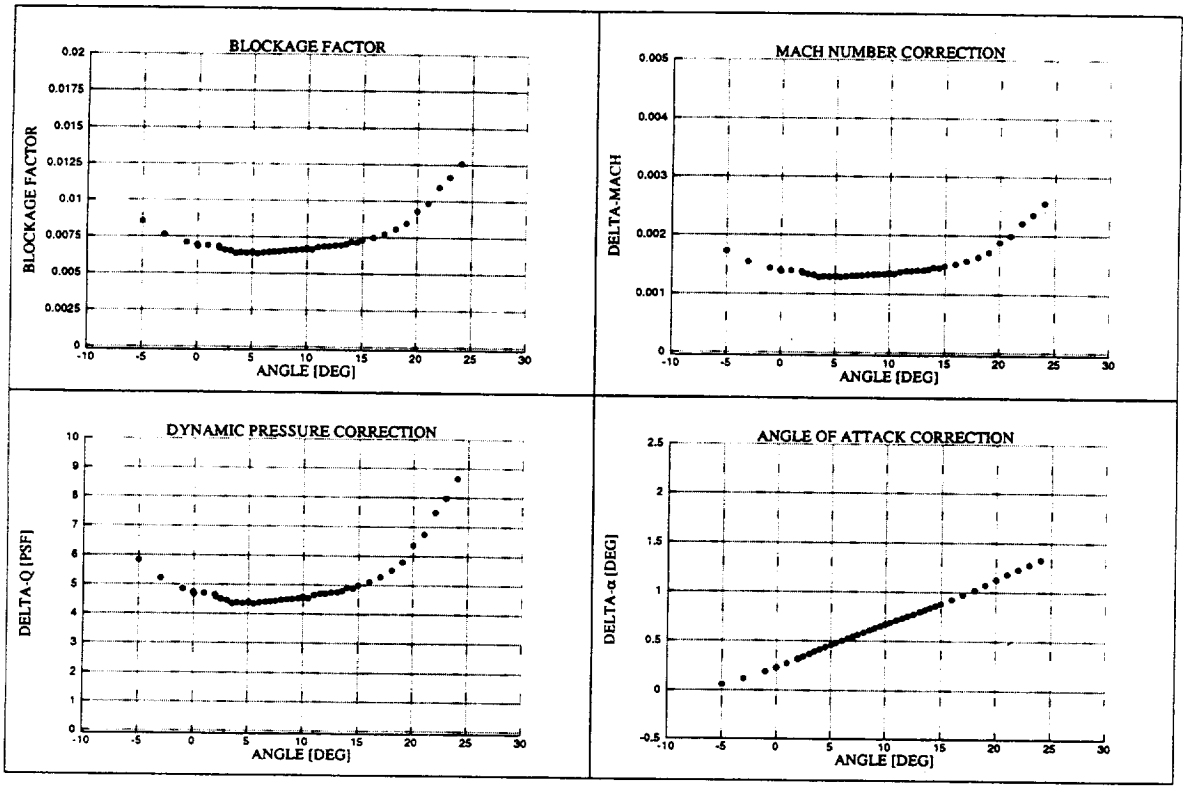


Figure 8. Wall interference corrections, WICS-NTF, semi-span model.
(Blockage corrections are averaged along fuselage center line; $\Delta\alpha$ is the weighted average along 3/4 chord line)

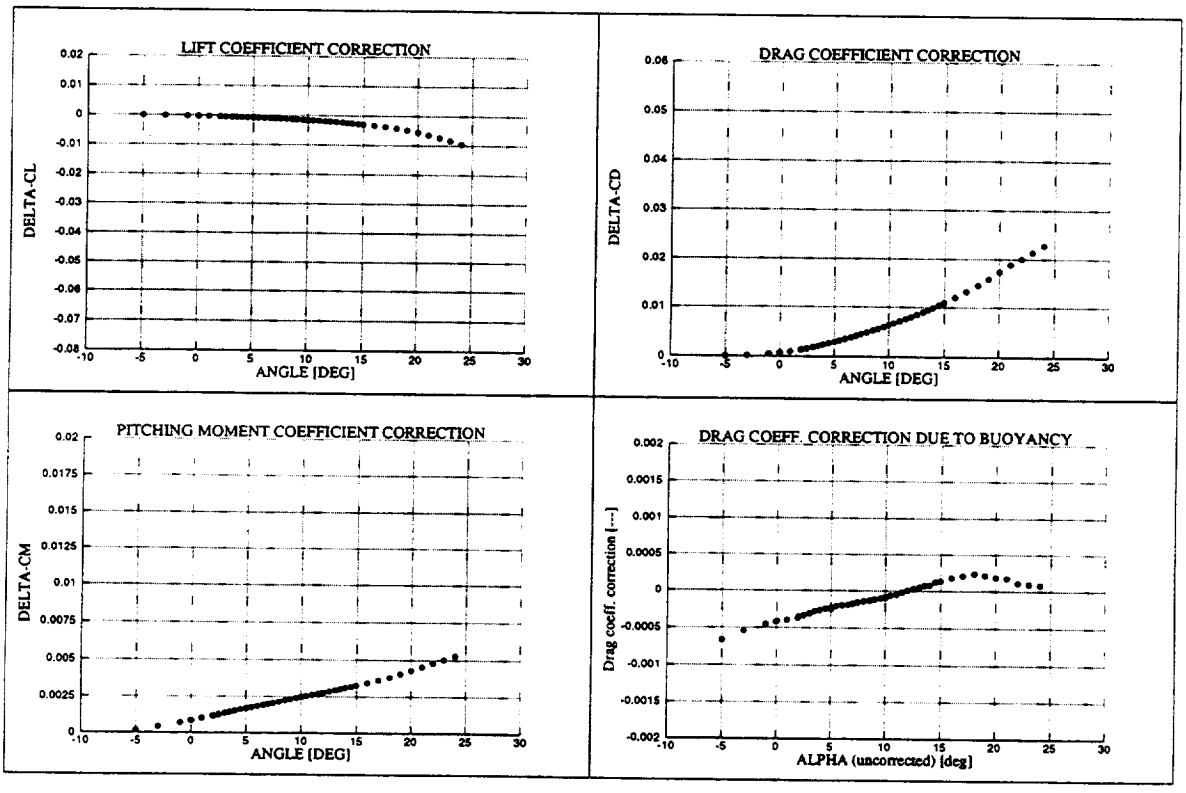


Figure 9. Wall interference coefficient corrections, WICS-NTF, semi-span model.
(Coefficient corrections due to wall-induced inclination of forces and moments, streamline curvature and buoyancy)

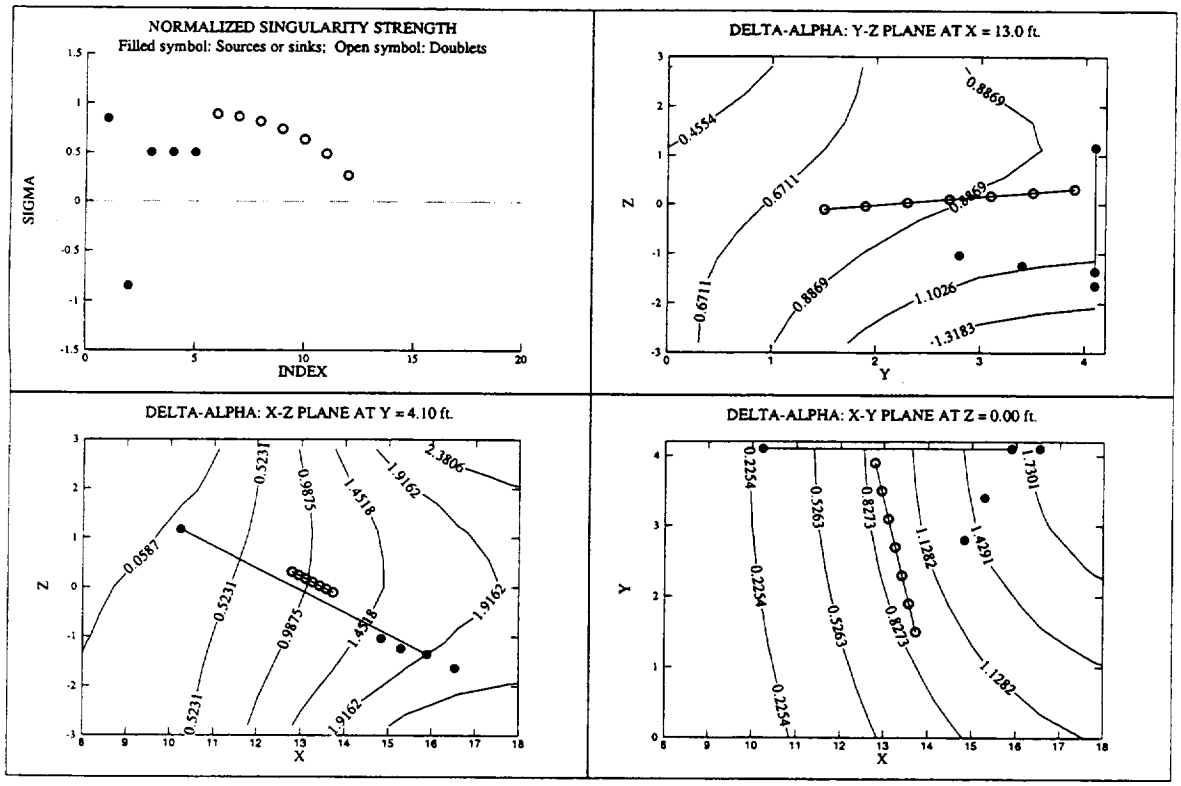


Figure 10. Contour plots of wall interference corrections, WICS-NTF.
(Contours of corrections are shown on three mutually orthogonal cutting planes; axis scales are independent)

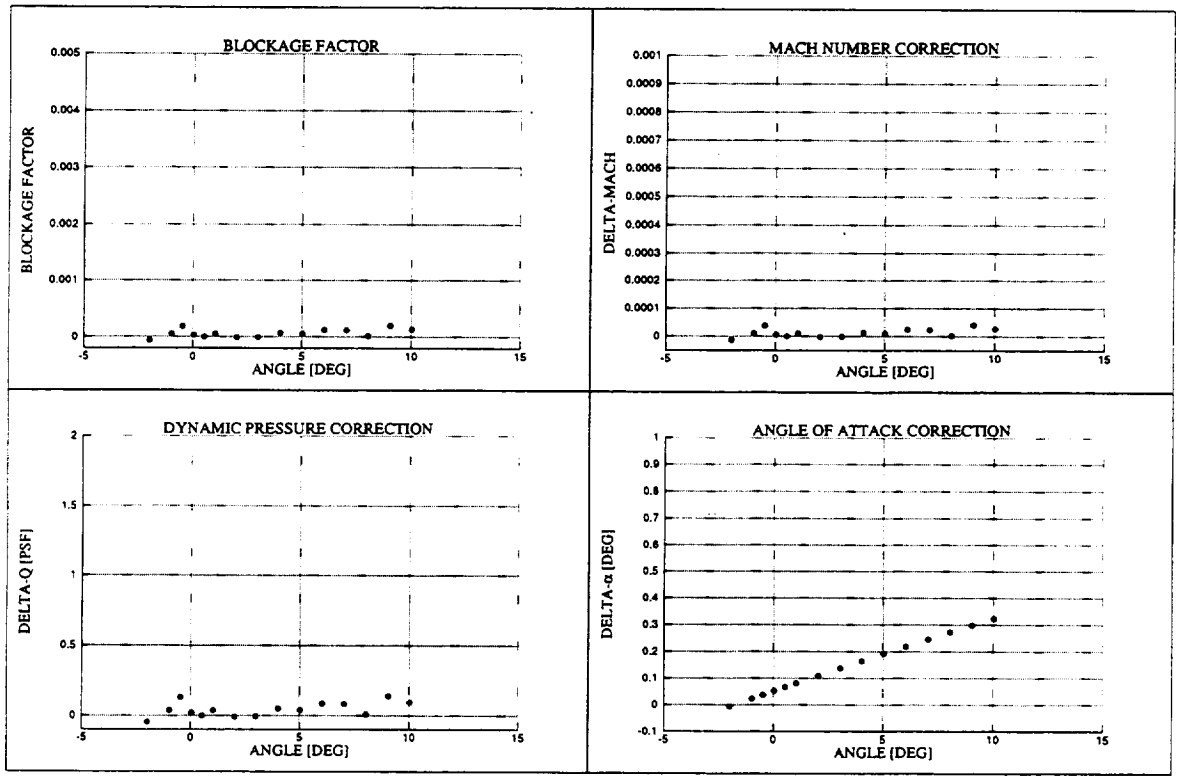


Figure 11. Wall interference corrections, WICS-NTF, full span model.
(Blockage corrections are averaged along fuselage center line; $\Delta\alpha$ is the weighted average along 3/4 chord line)

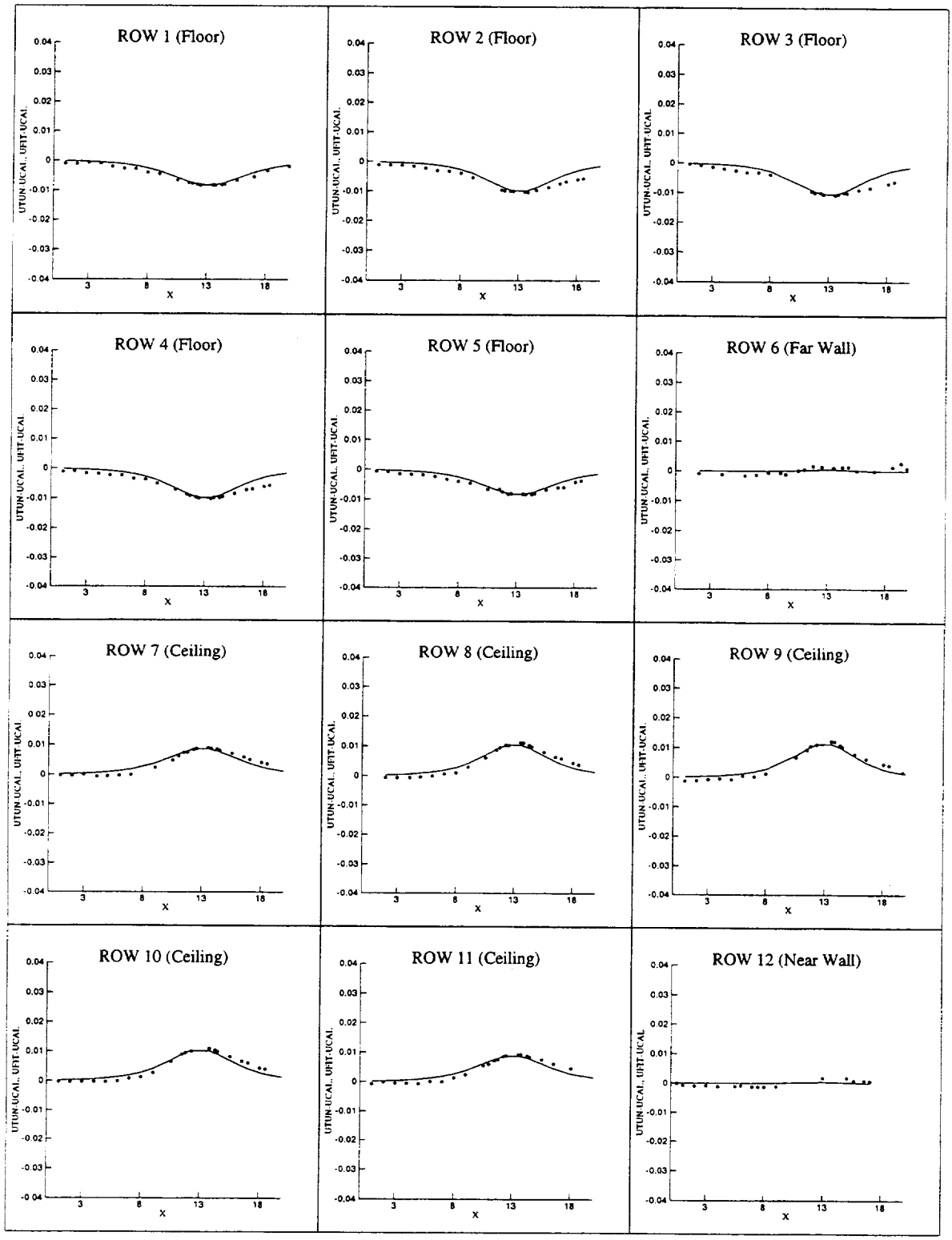


Figure 12. Wall signature, raw data and WICS-NTF fit, full span model at AOA=10°.
Symbols: UTUN-UCAL (Raw perturb. vel. minus tunnel empty vel.); Lines: UFIT-UCAL (WICS global fit of UTUN-UCAL).

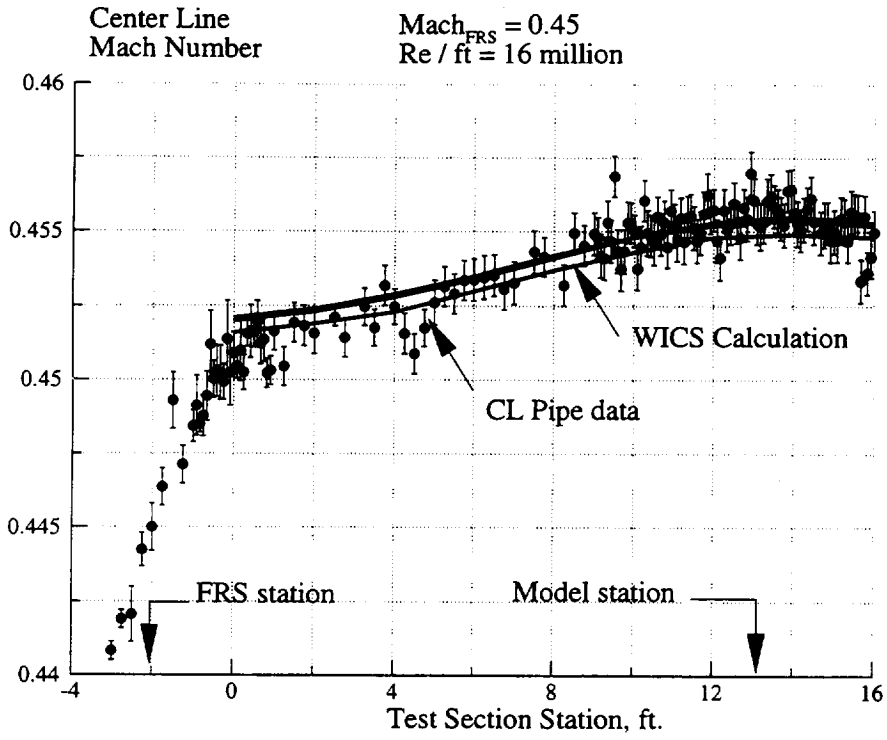


Figure 13. Center-line Mach number values from WICS-NTF and pipe data.

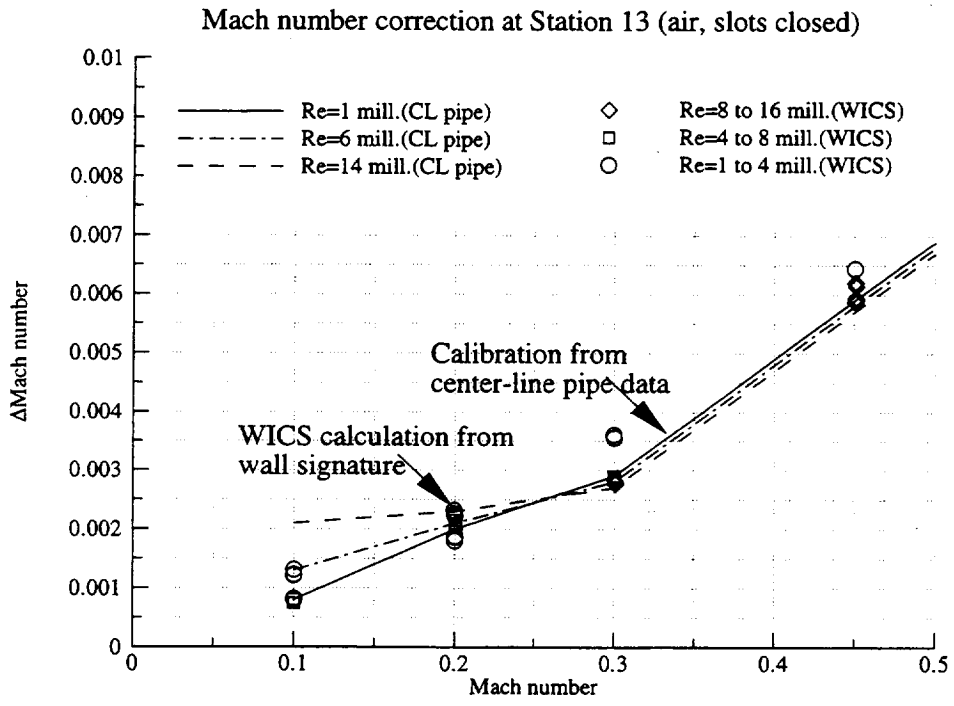


Figure 14. Mach number calibration with varying Mach and Reynolds numbers.

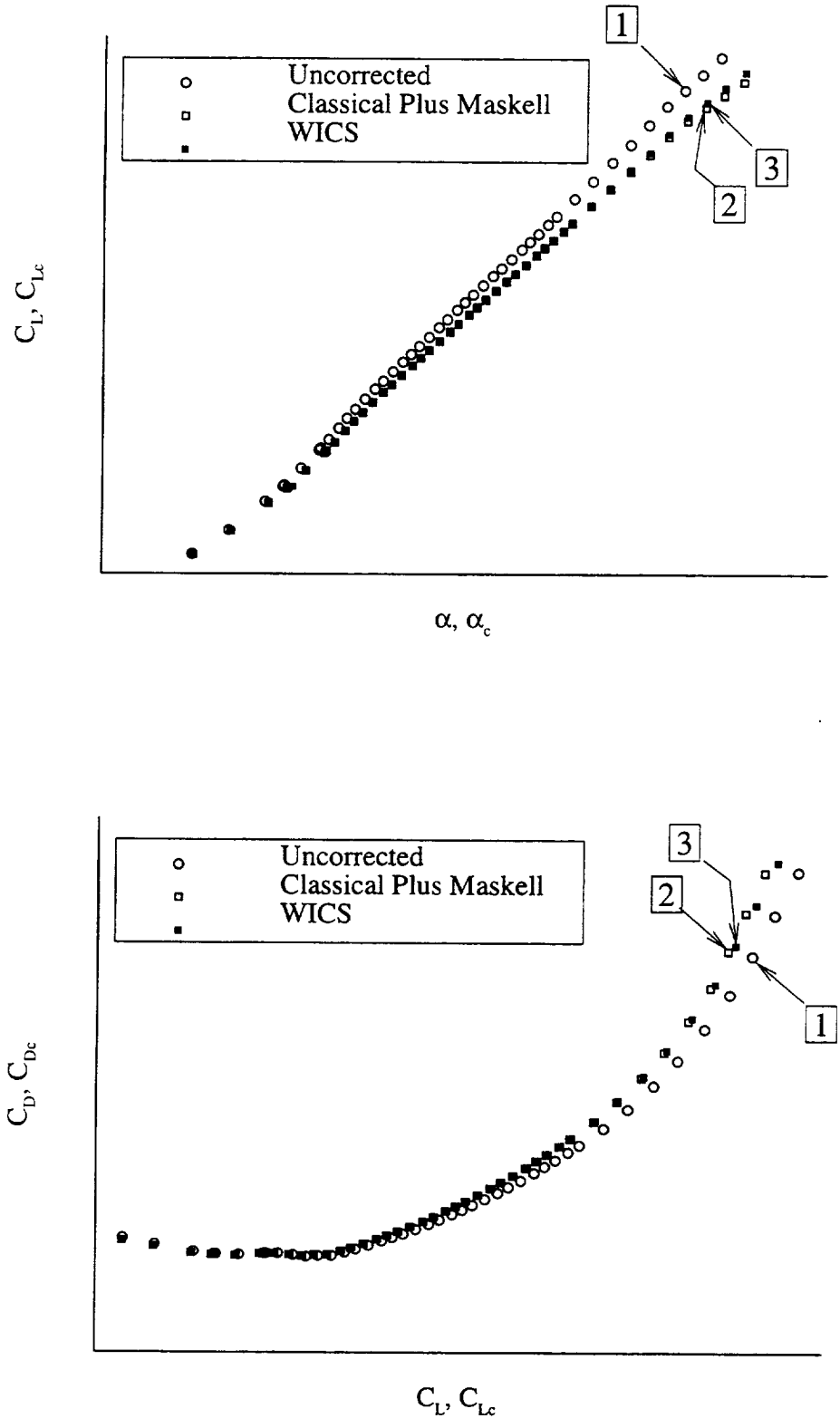


Figure 15. Points in the measurement (uncorrected) space and corresponding points in the corrected space (see text in paper for notations 1,2, and 3).

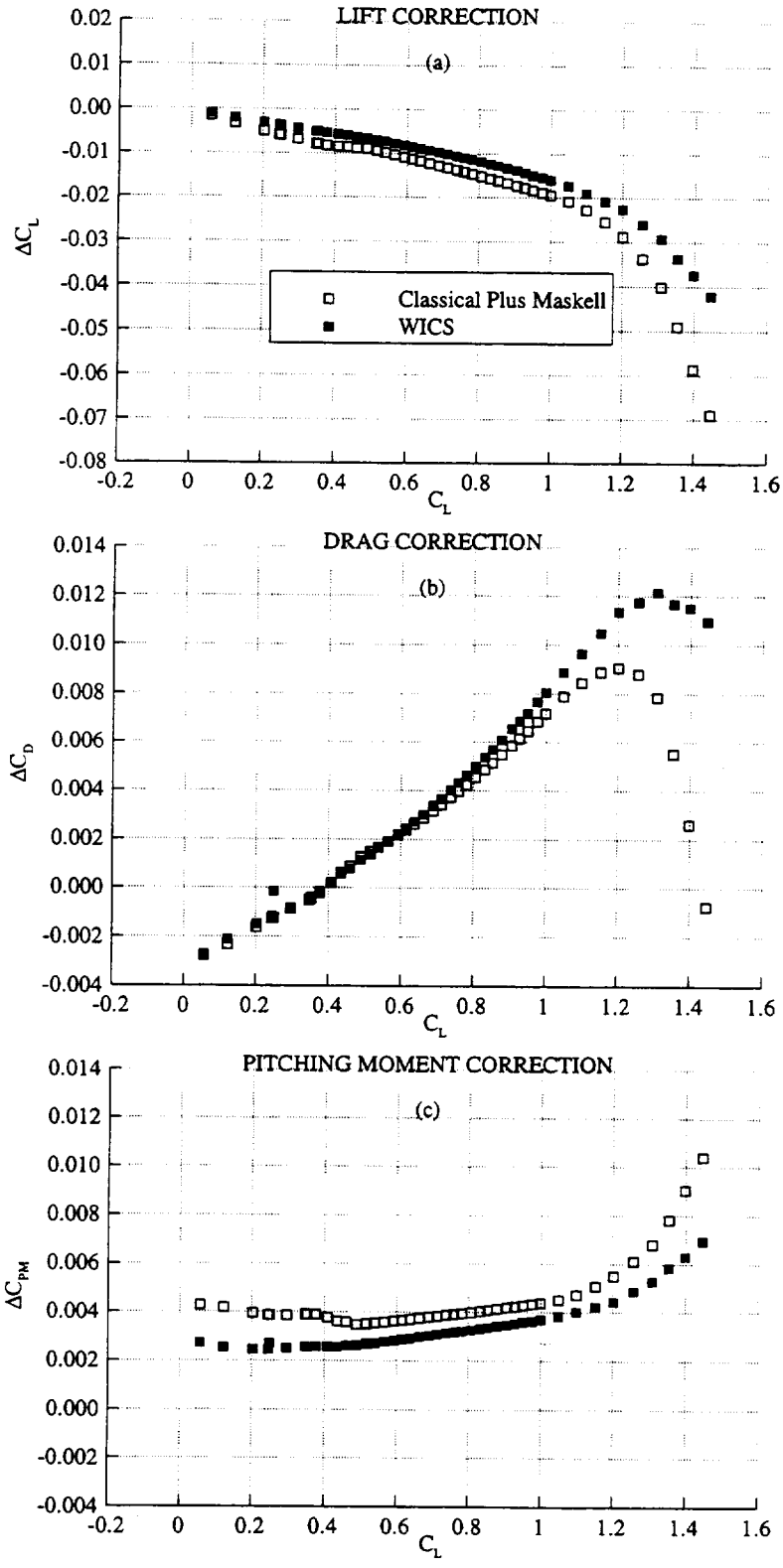


Figure 16. Comparison of corrections from WICS and classical plus Maskell methods.